

Radiative Transfer and Limb Darkening of Accretion Disks

Jun FUKUE and Chizuru AKIZUKI

Astronomical Institute, Osaka Kyoiku University, Asahigaoka, Kashiwara, Osaka 582-8582
fukue@cc.osaka-kyoiku.ac.jp

(Received 0 0; accepted 0 0)

Abstract

Transfer equation in a geometrically thin accretion disk is reexamined under the plane-parallel approximation with finite optical depth. Emergent intensity is analytically obtained in the cases with or without internal heating. For large or infinite optical depth, the emergent intensity exhibits a usual limb-darkening effect, where the intensity linearly changes as a function of the direction cosine. For small optical depth, on the other hand, the angle-dependence of the emergent intensity drastically changes. In the case without heating but with uniform incident radiation at the disk equator, the emergent intensity becomes isotropic for small optical depth. In the case with uniform internal heating, the limb brightening takes place for small optical depth. We also emphasize and discuss the limb-darkening effect in an accretion disk for several cases.

Key words: accretion, accretion disks — black holes — galaxies: active — radiative transfer — relativity

1. Introduction

Accretion disks are now widely believed to be energy sources in various active phenomena in the universe: in protoplanetary nebulae around young stellar objects, in cataclysmic variables and supersoft X-ray sources, in galactic X-ray binaries and microquasars, and in active galaxies and quasars. Accretion-disk models have been extensively studied during these three decades (see Kato et al. 1998 for a review).

Radiative transfer in the accretion disk has been investigated in relation to the structure of a static disk atmosphere and the spectral energy distribution from the disk surface (e.g., Meyer, Meyer-Hofmeister 1982; Cannizzo, Wheeler 1984; Křiž and Hubeny 1986; Shaviv, Wehrse 1986; Adam et al. 1988; Hubeny 1990; Ross et al. 1992; Artemova et al. 1996; Hubeny, Hubeny 1997, 1998; Hubeny et al. 2000, 2001; Davis et al. 2005; Hui et al. 2005). In many cases the diffusion approximation or Eddington one was employed; it provides a satisfactory description at large optical depth, although the emergent radiation field originates at optical depth of the order of unity. Furthermore, gray and non-gray models of accretion disks were constructed under numerical treatments (Křiž and Hubeny 1986; Shaviv and Wehrse 1986; Adam et al. 1988; Ross et al. 1992; Shimura and Takahara 1993; Hubeny, Hubeny 1997, 1998; Hubeny et al. 2000, 2001; Davis et al. 2005; Hui et al. 2005) and under analytical ones (Hubeny 1990; Artemova et al. 1996).

In these studies, however, the vertical movement and the mass loss were not considered. Hence, recently, in relation to the radiative disk wind, radiative transfer in a moving disk atmosphere was also investigated (e.g., Fukue 2005a, b, 2006a, b). In contrast to the static atmosphere, in the moving atmosphere the boundary condition at the

surface of zero optical depth should be modified (Fukue 2005a, b). Moreover, the usual Eddington approximation violates in the highly relativistic flow (Fukue 2005b; see also Turolla, Nobili 1988; Turolla et al. 1995; Dullemond 1999), and the velocity-dependent variable Eddington factor was proposed (Fukue 2006b).

In the usual studies of radiative transfer in the disk, the emergent intensity has not been fully obtained, since the attention were usually focused on the disk internal structure such as a temperature distribution. In addition, the effect of limb darkening has not been well examined except for a few cases relating to cataclysmic variables (e.g., Diaz et al. 1996; Wade, Hubeny 1998; see also Fukue 2000; Hui et al. 2005 for high energy cases).

In this paper, we thus reexamine radiative transfer in the accretion disk with *finite optical depth* under the plane-parallel approximation, and analytically obtain an emergent intensity for the cases with or without internal heating. Besides cataclysmic variables, we also emphasize and discuss the limb-darkening effect in an accretion disk for various cases.

In the next section we describe the basic equations. In section 3, we show analytical solutions. In section 4, we discuss several cases of accretion disk models, and emphasize the importance of the limb-darkening effect. The final section is devoted to concluding remarks.

2. Basic Equations

We here assume the followings: (i) The disk is steady and axisymmetric. (ii) It is also geometrically thin and plane parallel. (iii) As a closure relation, we use the Eddington approximation. (iv) The gray approximation, where the opacity does not depend on frequency, is adopted. (v) The viscous heating rate is concentrated

at the equator or uniform in the vertical direction.

The radiative transfer equations are given in several literatures (Chandrasekhar 1960; Mihalas 1970; Rybicki, Lightman 1979; Mihalas, Mihalas 1984; Shu 1991; Kato et al. 1998). For the plane-parallel geometry in the vertical direction (z), the frequency-integrated transfer equation, the zeroth moment equation, and the first moment equation become, respectively,

$$\cos\theta \frac{dI}{dz} = \rho \left[\frac{j}{4\pi} - (\kappa_{\text{abs}} + \kappa_{\text{sca}})I + \kappa_{\text{sca}} \frac{c}{4\pi} E \right], \quad (1)$$

$$\frac{dF}{dz} = \rho(j - c\kappa_{\text{abs}}E), \quad (2)$$

$$\frac{dP}{dz} = -\frac{\rho(\kappa_{\text{abs}} + \kappa_{\text{sca}})}{c} F, \quad (3)$$

where θ is the polar angle, I the frequency-integrated specific intensity, E the radiation energy density, F the vertical component of the radiative flux, P the zz -component of the radiation stress tensor, ρ the gas density, and c the speed of light. The mass emissivity j and opacity κ_{abs} and κ_{sca} are assumed to be independent of the frequency (gray approximation).

For matter, the vertical momentum balance and energy equation are, respectively,

$$0 = -\frac{d\psi}{dz} - \frac{1}{\rho} \frac{dp}{dz} + \frac{\kappa_{\text{abs}} + \kappa_{\text{sca}}}{c} F, \quad (4)$$

$$0 = q_{\text{vis}}^+ - \rho(j - c\kappa_{\text{abs}}E), \quad (5)$$

where ψ is the gravitational potential, p the gas pressure, and q_{vis}^+ the viscous-heating rate. In this paper, we do not solve the hydrostatic equilibrium (4). Generally speaking, when the contribution of the radiative flux is small, compared with the pressure gradient term, the gas pressure dominates in the atmosphere, and the density distribution will not be constant. When the radiative flux is strong, on the other hand, the radiation pressure dominates, and the density may be approximately constant throughout much of the disk. Anyway, we suppose that the density distribution would be adjusted so as to hold the hydrostatic equilibrium (4) through the main part of the disk atmosphere, under the radiative flux obtained later.

Using this energy equation (5) and introducing the optical depth, defined by

$$d\tau \equiv -\rho(\kappa_{\text{abs}} + \kappa_{\text{sca}}) dz, \quad (6)$$

we rewrite the radiative transfer equations:

$$\mu \frac{dI}{d\tau} = I - \frac{c}{4\pi} E - \frac{1}{4\pi} \frac{1}{\kappa_{\text{abs}} + \kappa_{\text{sca}}} \frac{q_{\text{vis}}^+}{\rho}, \quad (7)$$

$$\frac{dF}{d\tau} = -\frac{1}{\kappa_{\text{abs}} + \kappa_{\text{sca}}} \frac{q_{\text{vis}}^+}{\rho}, \quad (8)$$

$$c \frac{dP}{d\tau} = F, \quad (9)$$

$$cP = \frac{1}{3} cE, \quad (10)$$

where $\mu \equiv \cos\theta$. Final equation is the usual Eddington approximation.

As for the boundary condition at the disk surface of $\tau = 0$, we impose a usual condition:

$$3cP_s = cE_s = 2F_s \quad \text{at } \tau = 0, \quad (11)$$

where the subscript s denotes the values at the disk surface.

For the internal heating, we consider two extreme cases: (i) No heating ($q_{\text{vis}}^+ = 0$), where the viscous heating is concentrated at the disk equator and there is no heating source in the atmosphere. (ii) Uniform heating in the sense that $q_{\text{vis}}^+ / (\kappa_{\text{abs}} + \kappa_{\text{sca}}) \rho = \text{constant}$. The latter case means that the kinematic viscosity ν is constant in the vertical direction, since $q_{\text{vis}}^+ / \rho = \nu (rd\Omega/dr)^2$, as long as the opacities are constant.

Finally, the disk total optical depth becomes

$$\tau_0 = -\int_H^0 \rho(\kappa_{\text{abs}} + \kappa_{\text{sca}}) dz, \quad (12)$$

where H is the disk half-thickness.

3. Analytical Solutions

Except for the emergent intensity I , several analytical expressions for moments as well as temperature distributions were obtained by several researchers (e.g., Laor, Netzer 1989; Hubeny et al. 2005; Artemova et al. 1996). For the completeness, we recalculate them as well as the intensity I .

3.1. No Heating Case

We first consider the case without heating in the disk atmosphere: $q_{\text{vis}}^+ = 0$, but with uniform incident intensity I_0 from the disk equator, where the viscous heating is assumed to be concentrated.

In this case, the analytical solutions of moment equations are easily given as

$$F = F_s = \pi I_0, \quad (13)$$

$$3cP = cE = 3F_s \left(\frac{2}{3} + \tau \right). \quad (14)$$

This is a familiar solution under the Milne-Eddington approximation for a plane-parallel geometry. It should be noted that the vertical radiative flux F is conserved, and equals to πI_0 at the disk equator.

Since we obtain the radiation energy density E in the explicit form, we can now integrate the radiative transfer equation (7). After several partial integrations, we obtain both an outward intensity $I(\tau, \mu)$ ($\mu > 0$) and an inward intensity $I(\tau, -\mu)$ as

$$I(\tau, \mu) = \frac{3F_s}{4\pi} \left[\frac{2}{3} + \tau + \mu - \left(\frac{2}{3} + \tau_0 + \mu \right) e^{(\tau - \tau_0)/\mu} \right] + I(\tau_0, \mu) e^{(\tau - \tau_0)/\mu}, \quad (15)$$

$$I(\tau, -\mu) = \frac{3F_s}{4\pi} \left[\frac{2}{3} + \tau - \mu - \left(\frac{2}{3} - \mu \right) e^{-\tau/\mu} \right], \quad (16)$$

where $I(\tau_0, \mu)$ is the boundary value at the midplane of the disk.

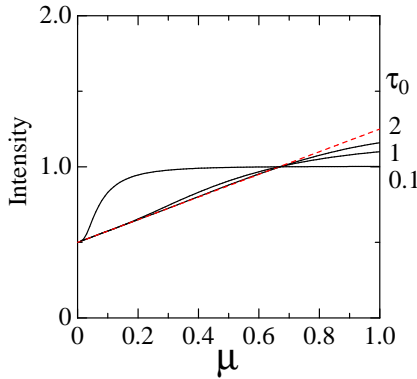


Fig. 1. Normalized emergent intensity as a function of μ for the case without heating. The numbers attached to each curve are values of τ_0 at the disk midplane. The dashed straight line is for the usual plane-parallel case with infinite optical depth.

In the geometrically thin disk with finite optical depth τ_0 and uniform incident intensity I_0 from the disk equator, the boundary value $I(\tau_0, \mu)$ of the outward intensity I consists of two parts:

$$I(\tau_0, \mu) = I_0 + I(\tau_0, -\mu), \quad (17)$$

where I_0 is the uniform incident intensity and $I(\tau_0, -\mu)$ is the *inward* intensity from the backside of the disk beyond the midplane. Determining $I(\tau_0, -\mu)$ from equation (16), we finally obtain the outward intensity as

$$\begin{aligned} I(\tau, \mu) &= \frac{3F_s}{4\pi} \left[\frac{2}{3} + \tau + \mu - 2\mu e^{(\tau-\tau_0)/\mu} \right. \\ &\quad \left. - \left(\frac{2}{3} - \mu \right) e^{(\tau-2\tau_0)/\mu} \right] + I_0 e^{(\tau-\tau_0)/\mu} \\ &= \frac{3F_s}{4\pi} \left[\frac{2}{3} + \tau + \mu + \left(\frac{4}{3} - 2\mu \right) e^{(\tau-\tau_0)/\mu} \right. \\ &\quad \left. - \left(\frac{2}{3} - \mu \right) e^{(\tau-2\tau_0)/\mu} \right], \end{aligned} \quad (18)$$

where we have used $F_s = \pi I_0$.

For sufficiently large optical depth τ_0 , this equation (18) reduces to the usual Milne-Eddington solution:

$$I = \frac{3F_s}{4\pi} \left(\frac{2}{3} + \tau + \mu \right). \quad (19)$$

Finally, the emergent intensity $I(0, \mu)$ emitted from the disk surface for the finite optical depth becomes

$$\begin{aligned} I(0, \mu) &= \frac{3F_s}{4\pi} \left[\frac{2}{3} + \mu + \left(\frac{4}{3} - 2\mu \right) e^{-\tau_0/\mu} \right. \\ &\quad \left. - \left(\frac{2}{3} - \mu \right) e^{-2\tau_0/\mu} \right]. \end{aligned} \quad (20)$$

In figure 1, the emergent intensity $I(0, \mu)$ normalized by the isotropic value \bar{I} ($= F_s/\pi$) is shown for several values

of τ_0 as a function of μ .

As is easily seen in figure 1, for large optical depth ($\tau_0 > 10$) the angle-dependence of the emergent intensity is very close to the case for a usual plane-parallel case with infinite optical depth. Therefore, the usual limb-darkening effect is seen. Namely, in the case of a semi-infinite disk with large optical depth, the energy density increases linearly with the optical depth in the atmosphere, and the temperature increases accordingly. As a result, an observer at a pole-on position of $\mu = 1$ will see deeper in the disk, where the temperature (and therefore, the source function) is larger than that observed by an observer at an edge-on position of $\mu = 0$. Thus, the observed intensity will be higher at $\mu = 1$. This is just a usual limb-darkening.

For small optical depth, however, the angle-dependence is drastically changed. When the optical depth is a few, the vertical intensity ($\mu \sim 1$) decreases due to the finiteness of the optical depth. That is, we cannot see the ‘deeper’ position in the atmosphere, compared with the case of a semi-infinite disk. Furthermore, when the optical depth is less than unity, the intensity in the direction of small μ increases, and the emergent intensity becomes isotropic with a uniform value I_0 at the disk equator; the limb-darkening effect disappears. Indeed, the limiting case of $\tau_0 \sim 0$, $I(0, \mu) \sim F_s/\pi$. That is, in this case of very small optical depth, the source function is dominated by the isotropic source at the midplane.

3.2. Uniform Heating Case

Now, we consider the case with uniform heating: $q_{\text{vis}}^+ / (\kappa_{\text{abs}} + \kappa_{\text{sca}}) \rho = \text{constant}$.

Integrating the equation (8) under the following boundary conditions:

$$\begin{aligned} F &= 0 & \text{at } \tau &= \tau_0, \\ F &= F_s & \text{at } \tau &= 0, \end{aligned} \quad (21)$$

we obtain

$$F = F_s \left(1 - \frac{\tau}{\tau_0} \right). \quad (22)$$

The radiative flux F linearly increases from 0 to the surface value F_s .

Substituting equation (22) into equation (9), and integrating the resultant equation under the boundary condition (11), we obtain

$$3cP = cE = 3F_s \left(\frac{2}{3} + \tau - \frac{\tau^2}{2\tau_0} \right). \quad (23)$$

This expression (23) for finite optical depth is seen in, e.g., Laor and Netzer (1989). A similar but more general expression was obtained by Hubeny (1990). In any case, this expression reduces to the Milne-Eddington solution for sufficiently large optical depth. In the case of finite optical depth, the radiation energy density and pressure decrease from the midplane to the surface in the quadratic form. It should be noted that at the midplane of the disk of $\tau = \tau_0$,

$$3cP = cE = 3F_s \left(\frac{2}{3} + \frac{\tau_0}{2} \right). \quad (24)$$

As already mentioned by Hubeny (1990), the energy density at the disk midplane is the half of the corresponding stellar atmospheric one. This is explained by the fact that the radiation from the disk midplane may escape equally to both sides of the disk.

Since we obtain the radiation energy density E in the explicit form (23), we can now integrate the radiative transfer equation (7). After several partial integrations, we obtain both an outward intensity $I(\tau, \mu)$ ($\mu > 0$) and an inward intensity $I(\tau, -\mu)$ as

$$I(\tau, \mu) = \frac{3F_s}{4\pi} \left[\frac{2}{3} + \tau + \mu + \frac{1}{\tau_0} \left(\frac{1}{3} - \frac{\tau^2}{2} - \mu\tau - \mu^2 \right) - \left(\frac{2}{3} + \frac{\tau_0}{2} + \frac{1}{3\tau_0} - \frac{\mu^2}{\tau_0} \right) e^{(\tau-\tau_0)/\mu} \right] + I(\tau_0, \mu) e^{(\tau-\tau_0)/\mu}, \quad (25)$$

$$I(\tau, -\mu) = \frac{3F_s}{4\pi} \left[\frac{2}{3} + \tau - \mu + \frac{1}{\tau_0} \left(\frac{1}{3} - \frac{\tau^2}{2} + \mu\tau - \mu^2 \right) - \left(\frac{2}{3} - \mu + \frac{1}{3\tau_0} - \frac{\mu^2}{\tau_0} \right) e^{-\tau/\mu} \right], \quad (26)$$

where $I(\tau_0, \mu)$ is the boundary value at the midplane of the disk.

In the case with uniform heating and without the incident intensity, the boundary value $I(\tau_0, \mu)$ of the outward intensity I is

$$I(\tau_0, \mu) = I(\tau_0, -\mu), \quad (27)$$

and we finally obtain the outward intensity as

$$I(\tau, \mu) = \frac{3F_s}{4\pi} \left[\frac{2}{3} + \tau + \mu + \frac{1}{\tau_0} \left(\frac{1}{3} - \frac{\tau^2}{2} - \mu\tau - \mu^2 \right) - \left(\frac{2}{3} - \mu + \frac{1}{3\tau_0} - \frac{\mu^2}{\tau_0} \right) e^{(\tau-2\tau_0)/\mu} \right]. \quad (28)$$

For sufficiently large optical depth τ_0 , this equation (28) also reduces to the usual Milne-Eddington solution (19).

Finally, the emergent intensity $I(0, \mu)$ emitted from the disk surface for the finite optical depth becomes

$$I(0, \mu) = \frac{3F_s}{4\pi} \left[\frac{2}{3} + \mu + \frac{1}{\tau_0} \left(\frac{1}{3} - \mu^2 \right) - \left(\frac{2}{3} - \mu + \frac{1}{3\tau_0} - \frac{\mu^2}{\tau_0} \right) e^{-2\tau_0/\mu} \right]. \quad (29)$$

In figure 2, the emergent intensity $I(0, \mu)$ normalized by the isotropic value $\bar{I} (= F_s/\pi)$ is shown for several values of τ_0 as a function of μ .

As is easily seen in figure 2, for large optical depth ($\tau_0 > 10$) the angle-dependence of the emergent intensity is very close to the case with a usual plane-parallel case with infinite optical depth. Therefore, the usual limb-darkening effect is seen, as already stated at the end of section 3.1.

For small optical depth, however, the angle-dependence

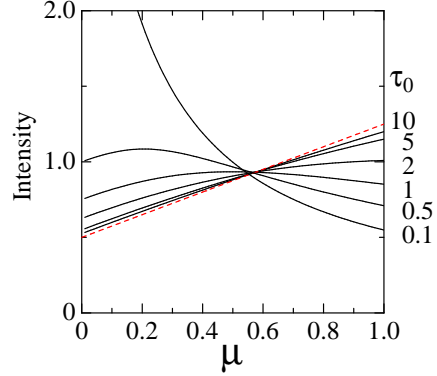


Fig. 2. Normalized emergent intensity as a function of μ for the case with uniform heating. The numbers attached on each curve are values of τ_0 at the disk midplane. The dashed straight line is for the usual plane-parallel case with infinite optical depth.

is drastically changed similar to the case without heating. In the vertical direction of $\mu \sim 1$, the emergent intensity decreases as the optical depth decreases. This is due to the finiteness of the optical depth. That is, we cannot see the ‘deeper’ position in the atmosphere, compared with the case of a semi-infinite disk. In the inclined direction of small μ , on the other hand, the emergent intensity becomes larger than that in the case of the infinite optical depth. Moreover, when the optical depth is less than unity, the emergent intensity for small μ is greater than unity: the *limb brightening* takes place. Indeed, in the limiting case of $\tau_0 \sim 0$, $I(0, \mu) \sim (F_s/\pi)/(2\mu)$. This is because that the path length is longer for such a case of small μ . That is, in this case for low optical depth, the source function is very uniform. This, coupled with the absence of an isotropic source at the midplane, is why the geometric effect (longer path length) is dominant and one finds limb ‘brightening’.

3.3. Validity of the Eddington Approximation

In this subsection, we briefly discuss the validity of the closure relation in the present treatment. In this paper, we have adopted the usual Eddington approximation, where the ratio of the radiation pressure to the energy density is fixed as $1/3$, to close the moment equations. As is well known, this approximation is correct in the limit of an isotropic radiation field. Hence, in the problem of limb-darkening, where the deviation from the isotropy is essential, this approximation is only approximately correct, although it is used in the usual Milne-Eddington approximation.

For example, let us suppose the case of a semi-infinite disk with an infinite optical depth τ_0 . In this case, we easily calculate the energy density as well as the radiation pressure from the derived intensity (19) of the Milne-Eddington solution. At the deeper position in the atmo-

sphere, where the integration is done in all directions, the re-calculated variables satisfy the condition of $P/E = 1/3$. However, at the surface of the disk, where the integration should be done in a semi-sphere, this is not true. At the surface of $\tau = 0$, we integrate the emergent intensity to yield:

$$cE = \frac{3F_s}{2} \int_0^1 \left(\frac{2}{3} + \mu \right) d\mu = 3F_s \frac{7}{12}, \quad (30)$$

$$cP = \frac{3F_s}{2} \int_0^1 \left(\frac{2}{3} + \mu \right) \mu^2 d\mu = \frac{1}{3} 3F_s \frac{17}{24}, \quad (31)$$

or $P/E = (1/3)(17/14)$. Hence, in the case under the usual limb-darkening effect, the ratio of the radiation pressure to the energy density is slightly larger than $1/3$ at the surface. This is just the peaking effect originated from the anisotropic radiation field near to the disk surface.

On the other hand, in the limb-brightening case of small optical depth with uniform heating, the situation is reversed. In this case, the ratio of the radiation pressure to the energy density becomes smaller than $1/3$, and the Eddington approximation holds approximately. This is also originated from the anisotropy, and may be called an *anti-peaking* effect. As is seen in figure 2, the limb-brightening becomes stronger and stronger for small optical depth. Hence, for such a case of very small optical depth, the Eddington approximation would not be good, although the qualitative properties would not be changed.

In order to obtain the intensity distribution more precisely, we, for example, introduce a variable Eddington factor, that is beyond the scope of the present paper.

4. Discussion

As was derived in the previous section, the emergent intensity I of the accretion disk depends on the disk total optical depth τ_0 as well as the direction cosine μ . The limb-darkening effect is considerably modified for small τ_0 , compared with the usual case for infinite optical depth. Even for the case with sufficiently large optical depth, limb darkening in the luminous accretion disk must be important, and should be examined more carefully.

In this section, we discuss several cases in turn, and call the attention to the importance of the limb-darkening effect.

4.1. Standard Disk

The optical depth at the midplane in the inner region of a geometrically thin standard disk (Shakura, Sunyaev 1973; see also Kato et al. 1998) is expressed as

$$\tau_0 = \frac{1}{2} \kappa \Sigma = 20\alpha^{-1} \dot{m}^{-1} \hat{r}^{3/2} \left(1 - \sqrt{\frac{3}{\hat{r}}} \right)^{-1}, \quad (32)$$

where κ is the electron scattering optical depth, α the viscous parameter, \dot{m} the mass accretion rate normalized by the critical rate \dot{M} ($= L_E/c^2$), L_E being the Eddington luminosity of the central object, \hat{r} the radius normalized by the Schwarzschild radius r_g ($= 2GM/c^2$).

This optical depth becomes small for large \dot{m} and/or small \hat{r} . For a slightly large accretion rate, inside some critical radius

$$r_{\text{cr}} = 2\dot{m}, \quad (33)$$

the disk shifts to a supercritical regime, whereas the disk is a standard regime outside r_{cr} (Fukue 2004). At this critical radius, the optical depth becomes

$$\tau_{\text{cr}} \sim 57\alpha^{-1} \dot{m}^{1/2}. \quad (34)$$

Hence, in a usual situation the optical depth of the inner region of the standard disk is greater than several tens.

In such a situation, however, due to a usual limb-darkening effect for semi-infinite medium, the emergent radiation toward the pole-on direction is enhanced by 20 percent, while the emergent radiation seen from the edge-on direction diminishes by 50 percent. Thus, in calculating the flux and spectrum of the standard disk, we carefully consider the limb-darkening effect.

In the region inside the inner edge at $3r_g$, the disk gas freely falls toward the central black hole, and the surface density (i.e., the disk optical depth) quickly drops. Hence, the emergent spectrum from the innermost region inside the inner edge would be greatly modified from the optically thick case and the optically thin one.

4.2. Supercritical Disk

In the supercritical accretion disk, where the mass accretion rate exceeds the critical rate, the expression for the disk optical depth is changed. For example, in the self-similar model without mass loss (Fukue 2000), the optical depth at the midplane of the disk is

$$\tau_0 = \frac{\kappa \dot{M}}{4\pi c_1 \alpha} \frac{1}{\sqrt{GMr}} = \frac{\dot{m}}{\sqrt{2}c_1 \alpha} \frac{1}{\hat{r}}, \quad (35)$$

where c_1 is a coefficient of the order of unity. At the critical radius, the disk optical depth is

$$\tau_{\text{cr}} \sim \frac{1}{2c_1 \alpha} \dot{m}^{1/2}. \quad (36)$$

In the critical accretion disk (Fukue 2004), where the mass accretion rate exceeds the critical one, but the excess mass is expelled by the wind mass loss, the optical depth at the midplane of the disk is

$$\tau_0 = \frac{16\sqrt{6}}{\alpha} \hat{r}^{1/2} = 39.2\alpha^{-1} \hat{r}^{1/2}. \quad (37)$$

At the critical radius, the disk optical depth is

$$\tau_{\text{cr}} \sim 55\alpha^{-1} \dot{m}^{1/2}. \quad (38)$$

Hence, in a usual situation the optical depth of the supercritical/critical disk is also greater than several tens.

In such a situation, however, the usual limb-darkening effect for semi-infinite medium is also important (see Fukue 2000). In addition to the limb-darkening effect, the geometrical effects, such as a *projection effect* and a *self-occultation*, should be considered in calculating the flux and spectrum of the supercritical disk (e.g., Fukue 2000; Watarai et al. 2005; Kawata et al. 2006).

4.3. Disk Corona and ADAF

If a luminous disk is sandwiched by a disk corona, the situation is similar to the case without heating, but with the incident intensity from the midplane. Hence, when the optical depth of the corona is sufficiently smaller than unity, the emergent intensity is just that of the disk, except for a very small direction cosine. However, when the optical depth of the corona is a few, limb darkening takes place, and the emergent intensity toward the edge-on direction remarkably reduces.

On the other hand, if the accretion rate is quite small, and the inner region of the disk becomes an optically-thin advection dominated state (ADAF), the situation is similar to the case with internal heating, although, rigorously speaking, the plane-parallel approximation may be invalid. When the optical depth of an ADAF region is sufficiently smaller than unity, the limb brightening would take place.

In both cases with hot gas, however, the effect of the Compton scattering may be important. Hence, the angle dependence of the intensity would be modified by the angle dependence of the Compton scattering, and the transfer problem should be treated more carefully.

In addition, in the latter case of ADAF, the accretion flow is supposed to be conical or spherical. Hence, when the opening angle is small, the limb brightening would qualitatively take place. When the opening angle is large, on the other hand, the extension of the emitting region is large, and the angle dependence of the emergent intensity would become much more complicated than the present simple case.

4.4. Relativistic Disk

In the case of the relativistic standard disk (e.g., Novikov, Thorne 1973; Page, Thorne 1974), the situation is similar to the non-relativistic case. However, the direction cosine of the local emergent intensity in the disk to the observer is changed by two additional reasons: (i) the light trajectory is bent by the space-time curvature, and (ii) the emission from the gas rotating around a black hole suffers from the special relativistic aberration. Limb-darkening effect in the comoving frame on the spectral energy distribution (SED) from the relativistic accretion disk was considered by, e.g., Fu and Taam (1990) and Gierliński et al. (2001).

Recently, due to submilliarcsecond astrometry, imaging of a black-hole *silhouette* is expected to become possible in the near future at infrared and submillimetre wavelengths. The “photographs” of relativistic accretion disks around a black hole have been obtained by many researchers (Luminet 1979; Fukue, Yokoyama 1988; Karas et al. 1992; Jaroszyński et al. 1992; Fanton et al. 1997; Fukue 2003; Takahashi 2004, 2005). In these studies, however, the usual limb darkening was not considered.

Examples of silhouettes of a dressed black hole are shown in figures 3 and 4. In figure 3 an edge-on view with inclination angle of 80° is shown, while a pole-on view is expressed in figure 4. In both figures, the left pan-

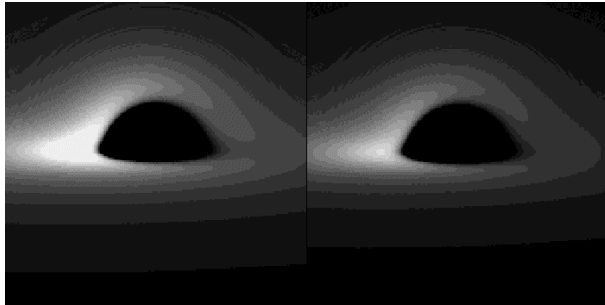


Fig. 3. Edge-on view of a dressed black hole without (left panel) and with (right panel) limb darkening. The inclination angle is 80° .

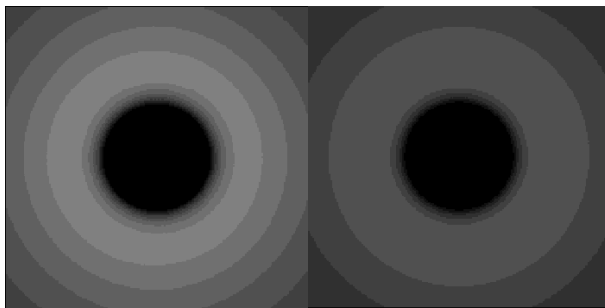


Fig. 4. Pole-on view of a dressed black hole without (left panel) and with (right panel) limb darkening. The inclination angle is 0° .

els are for the case without limb darkening, whereas the right panels are for the case with limb darkening.

In the edge-on view (figure 3), the image of a limb-darkening disk darkens as expected. This is due mainly to the usual limb-darkening effect for small direction cosine. Surprisingly, on the other hand, in the pole-on view (figure 4), the image of a limb-darkening disk also darkens! This is because that the local direction cosine becomes small due to the light aberration associated with the disk rotation.

Thus, in calculating spectra and observed fluxes of relativistic disks as well as in taking black hole silhouettes, we should carefully consider limb darkening. For example, besides Fu and Taam (1990) and Gierliński et al. (2001), Hui et al. (2005) discussed limb darkening in some details in their non-LTE calculation of accretion disk spectra around intermediate-mass black holes.

5. Concluding Remarks

In this paper we analytically solve the radiative transfer problem of a geometrically thin accretion disk with finite optical depth, and obtain analytical expressions for emergent intensity from the surface of the disk. For small optical depth, the angle-dependence of the emergent intensity drastically changes from the case with large optical depth. In the case without heating but with uniform incident radiation at the disk equator, the emergent intensity

becomes isotropic for small optical depth. In the case with uniform internal heating, the limb brightening takes place for small optical depth. We also emphasize the importance of limb darkening in the accretion disk study, and discuss several cases, including relativistic silhouettes.

In the calculation of spectra from, e.g., cataclysmic variables, the effect of limb darkening was considered (e.g., Diaz et al. 1996; Wade, Hubeny 1998). In the cases of high energy and relativistic regimes, we should also consider limb darkening (cf. Hui et al. 2005).

In addition, if there exist intense radiation sources, such as neutron stars or radiating jets, irradiation takes place and the outer boundary condition changes (e.g., Hubeny 1990). In such cases under strong incident radiation, limb brightening may occur (cf. Stibbs 1971), even for large optical depth.

Finally, if there exists mass loss from the disk surface, the radiative transfer problem becomes much more complicated. In order to examine spectra, fluxes, eclipsing light curves, we must calculate the emergent intensity analytically or numerically.

This work has been supported in part by a Grant-in-Aid for Scientific Research (18540240 J.F.) of the Ministry of Education, Culture, Sports, Science and Technology.

References

- Adam, J., Störzer, H., Shaviv, G., & Wehrse, R. 1988, *A&A*, 193, L1
- Chandrasekhar, S. 1960, *Radiative Transfer* (New York: Dover Publishing, Inc.)
- Cannizzo, J. K., & Wheeler, J. C. 1984, *ApJS*, 55, 367
- Davis, S. W., Blaes, O. M., Hubeny, I., & Turner, N. J. 2005, *ApJ*, 621, 372
- Diaz, M. P., Wade, R. A., & Hubeny, I. 1996, *ApJ*, 459, 236
- Dullemond, C.P. 1999, *A&A*, 343, 1030
- Fanton, C., Calvani, M., de Felice, F., & Čadež, A. 1997, *PASJ*, 49, 159
- Fu, A., & Taam, R.E. 1990, *ApJ*, 349, 553
- Fukue, J. 2000, *PASJ*, 52, 829
- Fukue, J. 2003, *PASJ*, 55, 155
- Fukue, J. 2004, *PASJ*, 56, 569
- Fukue, J. 2005a, *PASJ*, 57, 841
- Fukue, J. 2005b, *PASJ*, 57, 1023
- Fukue, J. 2006a, *PASJ*, 58, 187
- Fukue, J. 2006b, *PASJ*, 58, 461
- Fukue, J., & Yokoyama, T. 1988, *PASJ*, 40, 15
- Gierliński, M., Maciołek-Niedźwiecki, A., & Ebisawa, K. 2001, *MNRAS*, 325, 1253
- Hubeny, I. 1990, *ApJ*, 351, 632
- Hubeny, I., & Hubeny, V. 1997, *ApJ*, 484, L37
- Hubeny, I., & Hubeny, V. 1998, *ApJ*, 505, 558
- Hubeny, I., Agol, E., Blaes, O., & Krolik, J. H. 2000, *ApJ*, 533, 710
- Hubeny, I., Blaes, O., Krolik, J. H., & Agol, E. 2001, *ApJ*, 559, 680
- Hui, Y., Krolik, J. H. & Hubeny, I. 2005, 625, 913
- Jaroszyński, M., Wambsganss, J., & Paczyński, B. 1992, *ApJ*, 396, L65
- Karas, V., Vokrouhlický, D., & Polnarev, A.G. 1992, *MNRAS*, 259, 569
- Kato, S., Fukue, J., & Mineshige, S. 1998, *Black-Hole Accretion Disks* (Kyoto: Kyoto University Press)
- Kawata, A., Watarai, K., & Fukue, J. 2006, *PASJ*, 58, 477
- Křiž, S., & Hubeny, I. 1986, *BAIC*, 37, 129
- Laor, A., & Netzer, H. 1989, *MNRAS*, 238, 897
- Luminet, J.-P. 1979, *A&A*, 75, 228
- Meyer, F., & Meyer-Hofmeister, E. 1982, *A&A*, 106, 34
- Novikov, I. D., & Thorne, K. S. 1973, in *Black Holes*, ed. C. DeWitt and B.S. DeWitt (New York: Gordon and Breach)
- Page, D.N., & Thorne, K. S. 1974, *ApJ*, 191, 499
- Ross, R. R., Fabian, A. C., & Mineshige, S. 1992, *MNRAS*, 258, 189
- Shaviv, G., & Wehrse, R. 1986, *A&A*, 159, L5
- Shakura, N. I., & Sunyaev, R. A. 1973, *A&A*, 24, 337
- Shimura, T., & Takahara, F. 1993, *ApJ*, 440, 610
- Stibbs, D.W.N. 1971, *ApJ*, 168, 155
- Takahashi, R. 2004, *ApJ*, 611, 996
- Takahashi, R. 2005, *PASJ*, 57, 273
- Turolla, R., & Nobili, L. 1988, *MNRAS*, 235, 1273
- Turolla, R., Zampieri, L., & Nobili, L. 1995, *MNRAS*, 272, 625
- Wade, R.A., & Hubeny, I. 1998, *ApJ*, 509, 350
- Watarai, K., Ohsuga, K., Takahashi, R., & Fukue, J. 2005, *PASJ*, 57, 513